Journal of Biomedical Optics

SPIEDigitalLibrary.org/jbo

Nonlinear optical collagen cross-linking and mechanical stiffening: a possible photodynamic therapeutic approach to treating corneal ectasia

Dongyul Chai
Tibor Juhasz
Donald J. Brown
James V. Jester

SPIE

Nonlinear optical collagen cross-linking and mechanical stiffening: a possible photodynamic therapeutic approach to treating corneal ectasia

Dongyul Chai,[a] Tibor Juhasz,[a,b] Donald J. Brown,[a] and James V. Jester[a,b]
[a]University of California, Irvine, Gavin Herbert Eye Institute, Irvine, California 92697
[b]University of California, Irvine, Department of Biomedical Engineering, Irvine, California 92697

Abstract. In this study we test the hypothesis that nonlinear optical (NLO) multiphoton photoactivation of riboflavin using a focused femtosecond (FS) laser light can be used to induce cross-linking (CXL) and mechanically stiffen collagen as a potential clinical therapy for the treatment of keratoconus and corneal ectasia. Riboflavin-soaked, compressed collagen hydrogels are cross-linked using a FS laser tuned to 760 nm and set to either 100 mW (NLO CXL I) or 150 mW (NLO CXL II) of laser power. FS pulses are focused into the hydrogel using a 0.75 NA objective lens, and the hydrogel is three-dimensionally scanned. Measurement of hydrogel stiffness by indentation testing show that the calculated elastic modulus (E) values are significantly increased over twofold following NLO CXL I and II compared with baseline values ($P < 0.05$). Additionally, no significant differences are detected between NLO CXL and single photon, UVA CXL ($P > 0.05$). This data suggests that NLO CXL has a comparable effect to conventional UVA CXL in mechanically stiffening collagen and may provide a safe and effective approach to localize CXL at different regions and depths within the cornea. [DOI: 10.1117/1.JBO.18.3.038003]

Keywords: cross-linking; riboflavin; nonlinear optics; cornea; keratoconus.

Paper 12711RR received Nov. 2, 2012; revised manuscript received Feb. 13, 2013; accepted for publication Feb. 15, 2013; published online Mar. 20, 2013.

1 Introduction

The cornea is the outer, transparent part of the eye that provides two thirds of the refractive power for focusing light back to the retina. The cornea is composed of five tissue layers: the epithelium, Bowman's layer, stroma, Descemet's membrane, and endothelium. The corneal stroma represents 90% of the corneal thickness (~500 μm) and is comprised predominantly of a fibrous collagenous extracellular matrix that provides strength and shape to the cornea.

Corneal shape and refractive power are thought to be controlled by the mechanical properties of the stromal collagen and that regional differences in collagen organization influence local tissue mechanics. Past studies by Kokott suggested the presence of both a circumferential band of collagen that constrains the corneal curvature at the limbus, and a preferred nasal-temporal/superior-inferior orientation of deeper collagen layers that aligns with the extra ocular muscles.[1] Studies using x-ray diffraction have confirmed these earlier findings and shown a preferential alignment of collagen fibers in the mid–to posterior central cornea and an apparent tangential orientation in the corneal periphery.[2] More recent studies using nonlinear optical microscopy to image second-harmonic-generated (SHG) signals from collagen have also identified sutural or bow-string collagen fibers in the anterior stroma that insert into Bowman's layer and extensively intertwine with orthogonally arranged collagen fibers.[3] The degree of collagen intertwining has also been associated with increased mechanical stiffness of the anterior cornea, and that the mechanical weakening of the cornea as occurs in Keratoconus is associated with loss of sutural collagen fibers and decreased collagen intertwining.[3,4]

Keratoconus affects one in 2000 individuals in the United States and is the most common cause for corneal transplantation surgery.[5,6] A strategy for treating keratoconus has been introduced by Spoerl et al. that involves photoactivation of riboflavin by ultraviolet A light (UVA) inducing collagen cross-linking (CXL) leading to mechanical stiffening of the cornea.[7,8] Clinical results suggest that UVA CXL is effective in treating ectasia and that treatment substantially, if not permanently, halts the progression and delays the need for corneal transplantation.[9–11] Currently, UVA CXL is suggested for children and adolescents at the time of keratoconus diagnosis to prevent early progression of the disease.[12] In addition to treating other ectatic disorders such as post-LASIK ectasia, recent studies have shown that UVA CXL may have a wider range of therapeutic effects including enzymatic inhibition, antimicrobial activity for the treatment of corneal ulceration[13] and infectious keratitis.[14] Overall, UVA CXL therapy may substantially reduce the need for annually nearly 50,000 corneal transplant procedures performed in the United States.[9,12]

UVA CXL therapy involves an approach where the cornea is presoaked with riboflavin.[15] This currently requires the removal of the overlying corneal epithelium to allow penetration of riboflavin into the stroma, albeit alternative approaches not requiring epithelial removal are being intensively investigated.[16,17] Corneas are then exposed to 5.4 J/cm^2 of 370 nm UVA light for two to 30 min depending on the illumination intensity (3.0 to 45 mW/cm^2).[18,19] Photoactivation of riboflavin induces

Address all correspondence to: James V. Jester, University of California, Irvine, Gavin Herbert Eye Institute, 843 Health Science Road, Room 2036, Irvine, California 92697. Tel: 949-824-8047; Fax: 949-824-9626; E-mail: jjester@uci.edu

the formation of free radicals that interact with corneal proteins leading to covalent bonding within collagen fibrils.[20] Since generation of free radicals also causes cell death, riboflavin concentration, UVA irradiance, and treatment duration have all been selected to minimize cellular damage and protect the corneal endothelium.[10] These parameters effectively limit CXL to the anterior 300 μm of the corneal stroma[21] and also restrict UVA CXL therapy to corneas thicker than 400 microns. Alternative UVA CXL protocols that either preswell the cornea or reduce radiance exposure have been proposed for treating thin corneas,[13] however, endothelial damage even in thicker corneas has been reported and remains a concern.[22] Because of these concerns, it would be beneficial to develop methods that could improve both the lateral and axial control of corneal CXL to provide better safety and improve efficacy and expand therapy to treat other refractive disorders and corneal diseases.

Recently, femtosecond (FS) lasers have been used to photoactivate photosensitizers through the nonlinear optical (NLO), multiphoton processes within small focal volumes to provide high lateral and axial control of cross-linking for nano-fabrication (NLO CXL).[23] Studies show that NLO CXL can be used to create detailed three-dimensional (3-D) microstructures that integrate collagen and other proteins,[24,25] and that the material stiffness of these nanostructures can be modulated by laser dwell time.[26] Recently, NLO CXL has been used to stiffen bioengineered cardiac tissue, although the degree of mechanical stiffening was limited to less than 35% and not comparable to the therapeutically utilized UVA CXL of the cornea, which induces the mechanical stiffening of more than 200%.[27] In this study, we have evaluated the effectiveness of NLO CXL to mechanically stiffen compressed type I collagen hydrogels and compared the stiffening effect with that obtained using conventional UVA CXL.

2 Methods

2.1 *Determination of an Optimal Wavelength for Two-Photon Excitation of Riboflavin*

To determine the optimal wavelength for NLO riboflavin photoactivation, riboflavin fluorescent signal intensity as a function of femtosecond (FS) laser wavelength was measured. Riboflavin-5-phosphate (0.1%, Sigma-Aldrich, St. Louis, Missouri) in phosphate buffered saline (PBS; pH 7.3) was placed in a glass coverslip bottom Petri dish (MetTeK, Corporation, Ashland, Massachusetts) and mounted on the stage of a Zeiss, LSM 510 Meta laser scanning confocal microscope (Carl Zeiss, Jena, Germany). A 100 mW FS laser beam (Chameleon, Coherent Inc, Santa Clara, California) was then focused using a 20× (NA = 0.75) Zeiss Apochromat objective (Carl Zeiss), and the fluorescent signal was collected using the Meta Detector (Carl Zeiss) over the spectral range of 506 to 559 nm to include the peak signal (520 to 530 nm).[28] To appropriately set detector gain and offset and to provide maximum intensity of signal at peak excitation, the edge of the riboflavin solution in the Petri dish well was imaged providing the simultaneous detection of riboflavin fluorescence and negative background. Initial experiments indicated that peak excitation of riboflavin was obtained with 760 nm excitation at 100 mW of laser power. Gain and offset were then adjusted to achieve a full range of pixel intensity. Images were then taken at different FS laser wavelengths from 740 to 960 nm with the laser power adjusted to 100 mW at each wavelength maintaining the same gain and offset. The intensity of signal was then averaged over a 0.031 mm^2 rectangular region from the region of riboflavin fluorescence and negative background using Metamorph image processing software (Molecular Devices, Sunnyvale, California).

2.2 *Formation of Compressed Collagen Hydrogels*

Compressed collagen hydrogels were produced using methods previously described.[29] Briefly, acid soluble, rat-tail type I collagen (3 mg/ml) was neutralized with 1N NaOH (Acros, New Jersey), poured into a 24 well tissue culture plate (3 ml/well) and allowed to polymerize at 37°C in a 5% CO_2 humidified incubator for 30 min. Collagen hydrogels were then placed on top of a compression platform comprised of a #54 Whatman filter paper (GE Healthcare, Piscataway, New Jersey) having a 7.6-mm-diameter central window, which was used to transport the gel following compression. Beneath the transporting paper was a 50-μm nylon mesh (Sefar Filtration Inc., Depew, New York), an absorbing layer (two #1 Whatman filter papers, GE Healthcare) and a plastic plate as shown in Fig. 1(a). The hydrogel was then covered by a second nylon mesh, two #1 Whatman filter papers and a plastic plate, and then compressed by a 90-g mass for 5 min to squeeze out excessive water and form a thin collagen hydrogel with high collagen fiber density [Fig. 1(b)]. Compressed gel thickness was controlled by placing a 250-μm-thick spacer placed around the gel. Compressed gels were then moved for mechanical testing and collagen cross-linking by using the transporting paper to avoid possible damage [Fig. 1(c)] during transportation. No visible damage to the hydrogel during these movements was detected.

2.3 *Nonlinear Optical and UVA Collagen Cross-Linking*

To perform NLO and UVA CXL, gels were initially placed into a modified POC (Perfusion, Open and Closed)-R environmental chamber (Catalog #000000-1116-079, Carl Zeiss), as shown in

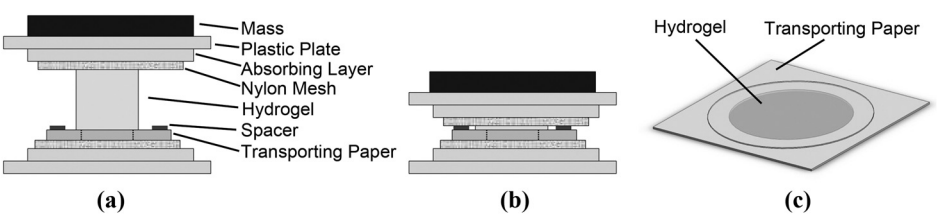

Fig. 1 (a) Formation of compressed hydrogel. Polymerized hydrogel was compressed on the window of a transporting paper by a mass between stacks of nylon mesh, absorbing layers, and plastic panel. Spacers were introduced to control compressed gel thickness. (b) Hydrogel after 5 min compression. (c) Hydrogel formed on transporting paper across the window. Note that homogenous hydrogel with dense structure of collagen fibers could be safely transported and indented through the window, avoiding wrinkle or folding.

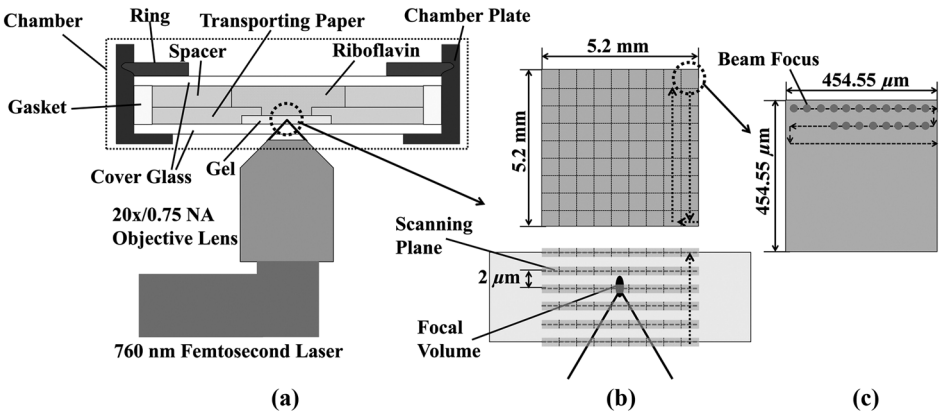

Fig. 2 Hydrogel scanning for NLO CXL. (a) Schematic of scanning hydrogel fixed with spacer in riboflavin solution-filled NLO CXL chamber using a femtosecond laser on a microscope. Assembly of hydrogel containing parts was sealed into chamber plate by screwing down the ring. (b) Schematic of axial (*Z*) scanning through hydrogel. Axial scanning was set to tile-scan over predetermined 5.2×5.2 mm area through whole gel thickness at 2 μm step. (c) Schematic of raster pattern within each tile. Focus of laser beam was moved at 28 cm/s in predetermined rectangular raster pattern.

Fig. 2(a). Hydrogels with transporting paper were placed onto the bottom 42-mm-diameter glass coverslip inside a 42 mm OD $\times$ 32 mm ID $\times$ 2 mm thick rubber gasket. The chamber was then filled with riboflavin (0.1% in PBS) and closed using a 42-mm-diameter glass coverslip and threaded stainless steel ring. Gel position was fixed by filling the space between transporting filter paper and upper cover glass with spacer (stack of Whatman #1 filter papers with 13-mm-diameter central window).

For NLO CXL the chamber was mounted onto the Zeiss LSM 510 Meta and a 760-nm FS laser beam was focused into gel through a $20\times/0.75$ NA objective lens (Zeiss). As shown in Fig. 2(b), the hydrogel was tile scanned over a 5.2×5.2 mm area through the thickness of the gel at 2 μm axial steps using the MultiTime function in the LSM software. As described in Fig. 2(c), each tile was raster scanned (512 lines) over a 455×455 μm area at 28 cm/s scan speed.

Hydrogels in environmental chambers used for control or UVA cross-linking were stored over night in riboflavin during NLO CXL of hydrogels to provide the same condition as NLO CXL gels. Hydrogels were then transferred to a 60-mm-diameter tissue culture dish (Becton Dickinson Labware, Franklin Lakes, New Jersey) containing fresh riboflavin solution and either exposed to 370-nm UVA light at an irradiance of 3.0 mW/cm^2 for 30 min or were mock treated for 30 min. The area of cross-linking was limited to 5.2×5.2 mm by placing a mask over the hydrogel.

2.4 *Measurement of Mechanical Stiffness*

To measure the mechanical properties of the compressed collagen gels before and after CXL, gels were clamped between an O-ring and gasket using two metal plates with a 7.6-mm-diameter central window (Fig. 3 and inset). The bottom plate was supported by a transparent cylinder and the device attached to a 3-D position control assembly as previously described.[21] A small amount of low viscosity silicon oil (Pure Silicone Fluid 1.5cSt, Clearco Products Co, Bensalem, Pennsylvania) was then applied to the surface of each gel to prevent dehydration and adhesion of the indenting probe tip to hydrogel surface prior to measurement of mechanical stiffness. Gels were indented at the center using a 250-μm-diameter round tip probe attached to a 5-μN resolution force transducer (F10, Harvard Apparatus, Holliston, Massachusetts). The axial position of the probe tip was controlled by a computer using LabVIEW 8.2 (National Instrument, Austin, Texas) through an electronic controller (ESP300, New Port Corporation, Irvine, California) so that the gel was indented at 20 μm/s through 1 mm depth

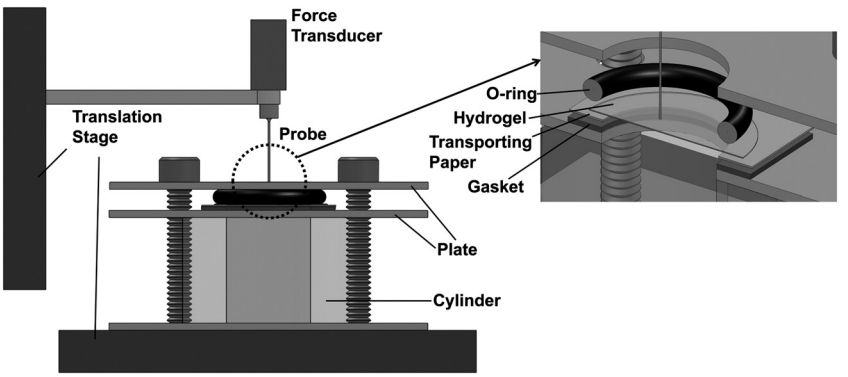

Fig. 3 Schematic of the indenting force-measurement system. Hydrogels were clamped between metal plates on cylinder on a XY positioning system using translation stages. 250-μm-diameter indenting probe was screwed into the tip of force transducer attached to *Z* positioning translation stage driven by a step motor. Hydrogel was clamped using *O*-ring and gasket and indented at the center of window (inlet).

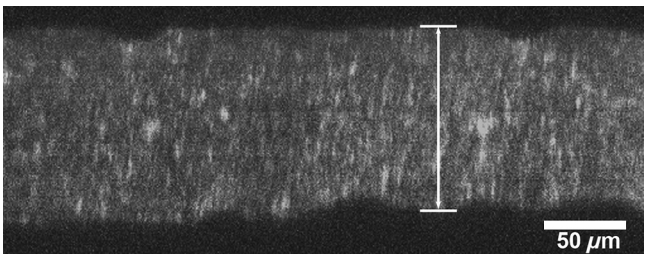

Fig. 4 Stack of SHG signal image. Thickness of hydrogel was determined by the distance between top and bottom surfaces (double-headed arrow).

over 10 cycles. The position of the tip and the signal from the force transducer were recorded every 0.05 s as previously described.[3]

Following indentation measurement, the collagen hydrogel thickness was microscopically measured by 3-D imaging the gel using NLO second harmonic generation (SHG) to detect collagen. Gels were placed on the LSM 510 Meta, and SHG signals were generated by a 800-nm FS laser beam using a 20×/0.75 NA objective (Zeiss). Forward scattered SHG signals were collected using a 400 ± 40 nm bandpass filter, and the hydrogels were axially scanned at 5 μm steps. Using LSM software, 3-D data sets were collected, reconstructed, and the thickness of the gels determined (Fig. 4). To estimate thickness, data sets were collected in five locations per gel, the center and 2 mm from the center at 0 deg, 90 deg, 180 deg, and 270 deg, and the average was calculated.

Elastic modulus was calculated using the modified Schwerin point-load solution:[30]

$$E = \frac{[f(v)]^3 a^2 P}{\delta^3 h},$$

$$f(v) \approx 1.049 - 0.146v - 0.158v^2,$$

where E = elastic modulus, δ = indentation displacement, v = Poisson's ratio, a = radius of window holding gel, h = gel thickness, and P = indenting force at the 10th cycle.

Poisson's ratio was assumed to be 0.5 as in the past study.[31] Elastic moduli before and after each treatment, E_{Baseline} and E_{post}, were calculated by inputting baseline and post-treatment measurements and thickness into the equation.

2.5 *Experimental Design*

A total of 12 compressed collagen hydrogels were manufactured for the study. Hydrogels gels were then divided into four groups: (1) not cross-linked, (2) conventional UVA CXL, (3) 760-nm FS light at 100 mW power (NLO CXL I), and 4) 760-nm FS light at 150 mW power (NLO CXL II). All hydrogels were soaked in 0.1% riboflavin in PBS for 30 min in a Petri dish. All hydrogels were also stored in the environmental chamber overnight to simulate conditions of NLO CXL and then transferred to a Petri dish to simulate conditions of UVA CXL. Mechanical stiffness and gel thickness was measured before and after treatment for all hydrogels. Each experimental run required approximately 12 h to complete, started and finished at the same time, and compared a NLO CXL to either a control or UVA CXL hydrogel. As a result, each hydrogel was treated exactly the same except for UVA, NLO, or mock light exposure.

2.6 *Statistics*

All measurements are reported as means ± standard deviations. The stiffening effect of each treatment was assessed by evaluating the statistical difference between E_{Baseline} and E_{post} values at 1-mm indenting depth using a repeated measures two-way ANOVA with a critical level of 0.05 (SigmaStat ver.3.1; Systat Software Inc., Point Richmond, California). The amount of stiffening was also assessed by comparing the ratio of elastic modulus, $E_{\text{post}}/E_{\text{Baseline}}$, between groups using a one-way ANOVA (SingmaStat ver 3.1) with the same critical level. The Holm-Sidak Method was used for both analyses.

3 Results

Figure 5(a) shows the riboflavin background and negative background with a rectangle on each side for analysis of fluorescence signal. Figure 5(b) shows the NLO-induced riboflavin fluorescence intensity as a function of FS wavelength normalized to the maximum value at 760 nm. It can be seen that riboflavin fluorescence was higher with FS excitation wavelengths of 740 and 760 nm with a peak at 760 nm. There was a marked reduction in intensity at FS wavelengths higher than 780 nm. These data indicated that 760 nm was the optimal wavelength to induce maximum NLO excitation of riboflavin in this experimental system, and the reduction of fluorescence from 780 nm wavelength is in agreement with the absorption over wavelength in the past study.[28] Although riboflavin is known to have a second absorption peak at 450 nm, a nonlinear absorption spectra peak above 760 was not detected.

Figure 6(a) is a representative indenting force curve for 10 cycles showing the viscoelastic properties of collagen hydrogels with hysteresis defined by the difference between loading and unloading curves. Comparing the indenting force at a 1 mm depth in each cycle, it can be seen that there was a noticeable difference between the first and second cycle that diminished with increasing cycle number and became negligible (less than 1%) by the 10th cycle. This suggests that a reasonably steady-state behavior was achieved, and the indenting force values from the 10th cycle could be used to calculate elastic modulus with minimum viscoelastic contribution. Figure 6(b)–6(d) shows representative indenting force curves from the 10th cycle of baseline and post-treatment measurements in UVA CXL, NLO CXL (I) and (II) groups, respectively.

Figure 7 shows the comparison in the average E values obtained before and after treatment for each group. First, there was no significant difference in the baseline measured E values between the different groups, although there was considerable variation between groups with average E values ranging from 0.92 ± 0.23 MPa to 1.53 ± 0.39 MPa. Second, photoactivation of riboflavin using either UVA or NLO at the two different powers showed significantly increased post-treatment E values compared to baseline ($P < 0.05$). Control hydrogels showed a slight increase in post-treatment E values, but this difference was not significant ($P > 0.05$). Because of the variation in the baseline E values between groups, a ratio between $E_{\text{post}}/E_{\text{Baseline}}$, was calculated and the differences in stiffening between groups compared. As shown in Fig. 8, the E value ratios for the UVA CXL and NLO CXL groups were significantly higher compared to the control group ($P < 0.05$), while no significant difference was detected between UVA CXL and NLO CXL ($P > 0.05$) groups.

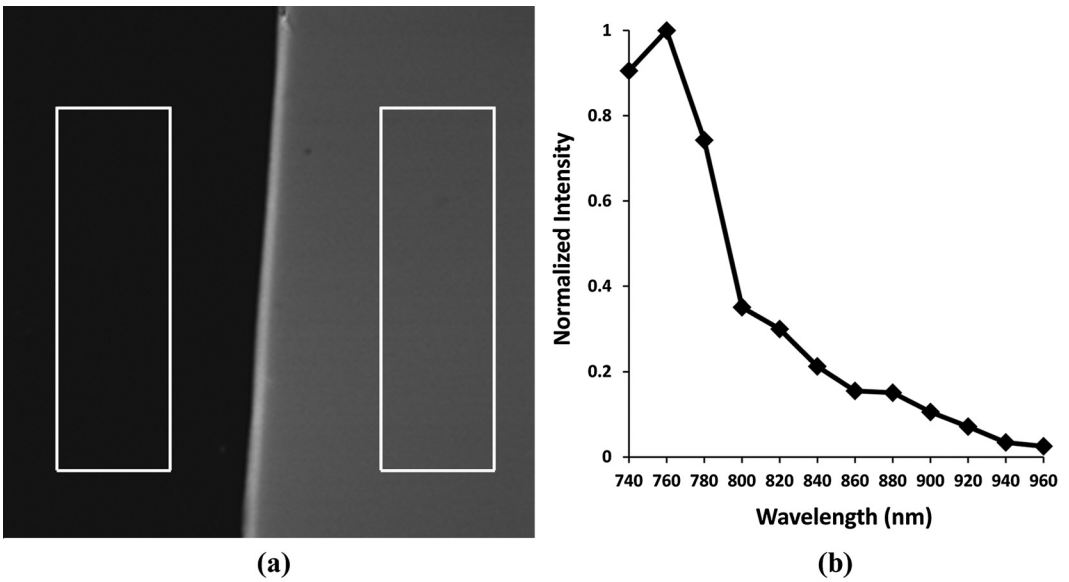

Fig. 5 (a) NLO fluorescence image of riboflavin (right) and negative background (left) over 506 to 559 nm spectrum following 100 mW femtosecond laser excitation with rectangles where intensity was averaged. (b) Normalized intensity of NLO excited fluorescence signal of riboflavin over excitation wavelengths. Intensity of riboflavin fluorescence signal was defined as the intensity difference between riboflavin and background signal. Note that 760 nm is the optimal wavelength for NLO CXL to induce the maximum excitation.

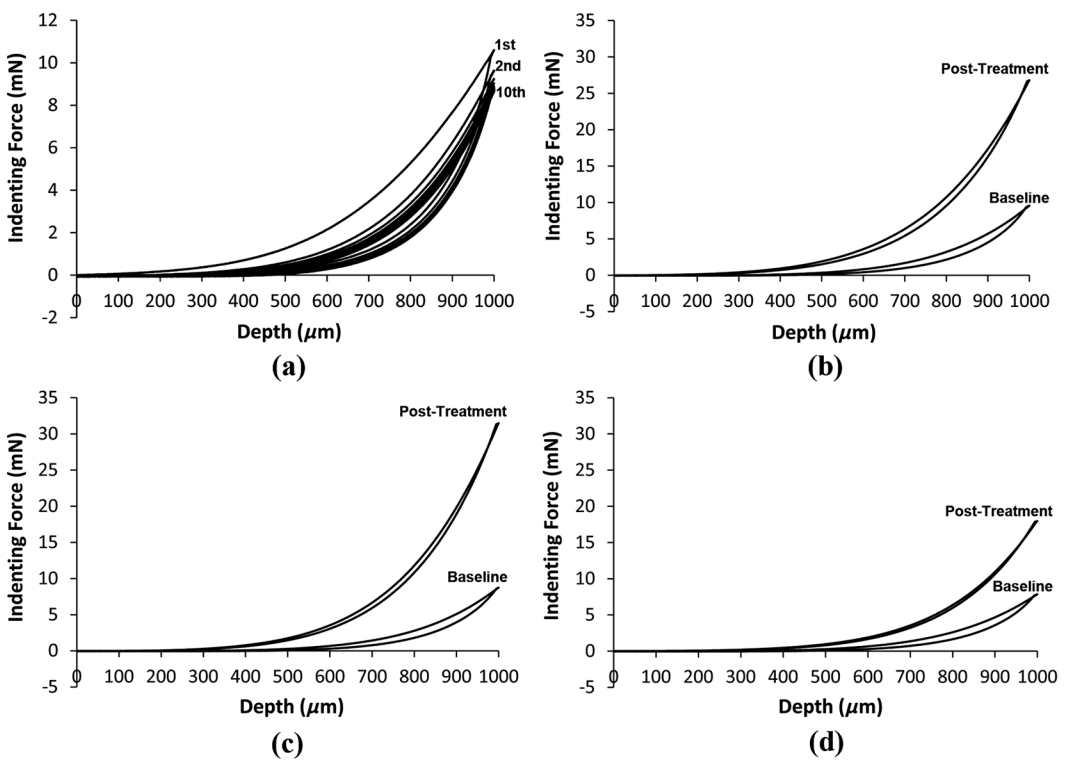

Fig. 6 (a) Representative indenting force curves for 10 cycles. Note that indenting force decreased with each cycle and was negligible at 10th cycle with minimum viscoelastic contribution. Indenting force curves at 10th cycles from baseline and post-treatment measurements in (b) UVA CXL, (c) NLO CXL (I), and (d) NLO CXL (II) groups. Note that indenting force from post-treatment was increased over twofold in each of (b), (c), and (d).

4 Discussion

Previous studies have shown that multiphoton processes can be used to activate photosensitizers and create detailed 3-D nanostructures,[24,25] with modified material stiffness characteristics based on FS laser dwell time.[26] It has also been demonstrated[27] that mechanical stiffening of bioengineered cardiac tissue can be achieved using a 5-KHz FS laser light focused using long focal distance lenses, although the degree of stiffening was less than 35%. The current report demonstrates for the first time that NLO photoactivation of riboflavin using 75-MHz FS laser focused using a high NA lens within a collagen hydrogel induces similar amount of collagen stiffening to that achieved by UVA CXL. Considering that NLO photoactivation of riboflavin is theoretically limited to the two photon focal volume, which for a

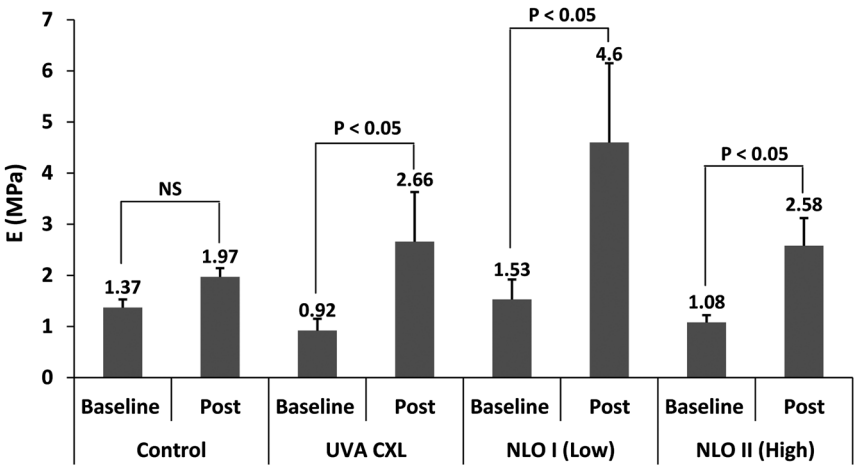

Fig. 7 Elastic moduli (mean + SD), E, of hydrogels before and after treatment in each group ($n = 3$) (NS: not significant). Note significant increase in E values in UVA and NLO CXL treated groups ($P < 0.05$), while there was no significant increase in control ($P > 0.05$).

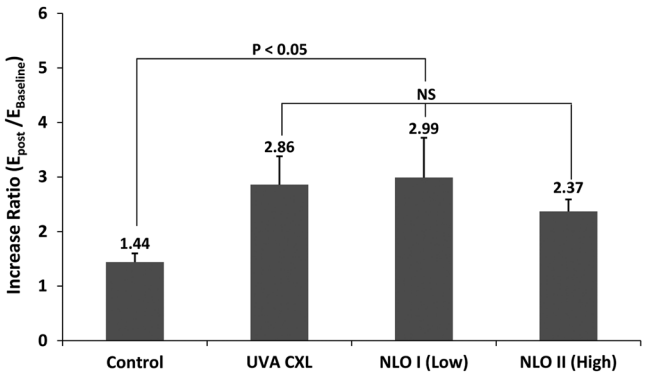

Fig. 8 Elastic modulus increase ratios (mean + SD), $E_{post}/E_{Baseline}$ of hydrogels in each group ($n = 3$) (NS: Not Significant). Increase ratios in UVA and NLO CXL treated groups were significantly different from that of control ($P < 0.05$). Also note that the increase ratios of NLO CXL groups are not significantly different from that of UVA CXL ($P > 0.05$).

0.75 NA lens is 0.5 μm lateral and 2.5 μm axial,[32] the current NLO CXL approach has the potential to address some of the limitations of UVA CXL. Specifically, NLO CXL can provide improved lateral and axial control of the volume of cornea that is cross-linked, thereby avoiding damage to underlying structures outside the focal volume of FS laser beam.

Improved control of CXL volume may become increasingly important as UVA CXL therapy gains wider acceptance. While UVA exposure levels during CXL was originally designed to avoid damage to the underlying corneal endothelium and the intraocular lens, recent cases of corneal endothelial failure following CXL in corneas thicker than 500 μm have been reported.[22] Additionally, a retrospective study of 350 patients identified 2.9% developing visually significant corneal edema presumed to be related to endothelial damage after receiving UVA CXL with stromal thicknesses greater than 400 μm.[33] Furthermore, in a prospective study of 12 patients an average 10% endothelial cell loss was identified after receiving UVA CXL with stromal thicknesses less than 400 μm.[34] While application of hypo-osmotic solutions to swell the cornea are recommended in such cases,[13] the effect of this treatment on endothelial cell density has not been evaluated.

The ability to control the CXL volume may also help to more safely expand the therapeutic domain to other ectatic disorders including post-LASIK ectasia. While the incidence of post-LASIK ectasia is low (<1%), it is a severe complication that can occur when the residual stromal bed thickness is not sufficient to maintain normal mechanical strength.[35] While UVA CXL at the time of surgery has been reported,[18] cross-linking of the residual bed might result in significant corneal endothelial cell damage and potentially damage the lens epithelium when residual bed thickness becomes less than 250 μm. By comparison, NLO CXL would be limited to the two-photon volume of the focusing lens, which can be precisely controlled by moving the lens respective to the cornea. In this manner the entire residual bed could undergo collagen cross-linking without exposing the corneal endothelium or underlying structures to the damaging effects of free radicals.

Another potential disadvantage of UVA CXL is that cross-linking is limited to the anterior corneal stroma.[21,36,37] Recent studies have shown that the collagen organization and mechanical properties of the corneal stroma show regional variations including a stiffer anterior stroma with collagen fiber intertwining and branching, a more compliant posterior stroma with collagen fibrils aligned along the major nasal/temporal and superior/inferior meridians, and a tangential collagen fibril orientation in the periphery.[2,3] How these different collagen fiber and fibril alignments control corneal mechanical properties and shape remain unknown. Although previous studies have shown that keratoconus corneas show structural changes in the anterior cornea,[4,38,39] whether cross-linking limited to the anterior 300 μm of stroma provides the most effective treatment is also not known. Since NLO CXL can be performed regionally and is not limited solely to the anterior cornea, the effects of different treatment strategies involving different depths, thicknesses, and patterns could be easily tested and may provide improved treatment outcomes.

In the current study, NLO CXL was performed using a Zeiss LSM 510 Meta, which limited the area available for photoactivation to a small 455 × 455 μm field of view using the Zeiss 20×/0.75 NA objective. A large field was successfully cross-linked by tiling over the collagen hydrogel using an automated XY translational stage and the built-in LSM software MultiTime macro function. Because of the slow y- and z-scanning rate and XY translational stage movement, cross-linking using this

system generally required 3 h to complete, compared to 2 to 30 min for UVA CXL, depending on the intensity of UVA light. Optimization of the scanning approach by adjusting scanning parameters—including two-photon focal volume, line speed, plane separation and intensity of laser beam—could markedly shorten the time for CXL, making this approach clinically feasible. However, increased scan speed will decrease FS laser dwell time leading to reduced generation of free radicals needed for cross-linking. However, it should be noted that NLO excitation of riboflavin can be achieved using concentrations of riboflavin above the clinically used 0.1% and at deeper depths in swollen corneas (~1 mm).[40] These findings suggest that decreased dwell time may be offset by increasing riboflavin concentration to generate free radicals.

In the current study, changes in material stiffness related to NLO and UVA CXL were assessed by tissue indentation as used in previous studies.[30,41] In addition, type I collagen hydrogels were used since type I collagen is the principal fibrous protein of the cornea and through compression can be reproducibly fabricated to generate a thin, homogeneous, dense collagen fiber structure similar to the cornea that was thin enough to facilitate NLO CXL throughout the corneal phantom. Since collagen organization in collagen hydrogels is random, tissue-indentation testing was used to measure the stiffening of collagen regardless of orientation. As shown in a past study,[42] extensiometry with unidirectional tensile measurements of materials with random collagen fibers orientation only assess the collagen fibers parallel to the stretching direction. On the other hand, indentation testing is more convenient when using thin collagen hydrogels as used in the current experiment. Considering the ratio of hydrogel thickness and indenting depth, 0.08 to 0.1, it can also be assumed that the force measured during indentation is from stretching of the hydrogel suggesting that indentation testing can be used as an alternative for measuring tensile modulus for small and thin materials.

5 Conclusions

This study shows that NLO photoactivation of riboflavin within collagen hydrogels can lead to mechanical stiffening of equal magnitude to that achieved using conventional UVA CXL. We propose that NLO CXL has the promise to provide higher lateral and axial control of corneal collagen cross-linking and a safe and effective treatment for corneal ectasia. Future work to develop an instrumental capable of rapidly inducing NLO CXL within the corneal stroma is needed to test this hypothesis.

Acknowledgments

This study is supported by NIH Infrastructure Grant EY019719, EY018665; The Discovery Eye Foundation, Research to Prevent Blindness, Inc, The Skirball Program in Molecular Ophthalmology.

References

1. W. Kokott, "Ubermechanisch-funktionelle strikturen des auges.," *Albrecht. von Graefes Arch. Ophthalmol.* **138**(4), 424–485 (1938).
2. M. Abahussin et al., "3D collagen orientation study of the human cornea using X-ray diffraction and femtosecond laser technology," *Invest. Ophthalmol. Visual Sci.* **50**(11), 5159–5164 (2009).
3. M. Winkler et al., "Nonlinear optical macroscopic assessment of 3-D corneal collagen organization and axial biomechanics," *Invest. Ophthalmol. Visual Sci.* **52**(12), 8818–8827 (2011).
4. N. Morishige et al., "Second-harmonic imaging microscopy of normal human and keratoconus cornea," *Invest. Ophthalmol. Visual Sci.* **48**(3), 1087–1094 (2007).
5. E. B. A. o. America, 2009 Eye Banking Statistical Report, Eye Bank Association of America, Washington, DC, http://www.restoresight.org/ (2009).
6. W. J. Cunningham et al., "Trends in the distribution of donor corneal tissue and indications for corneal transplantation: the New Zealand National Eye Bank Study 2000–2009," *Clin. Exp. Ophthalmol.* **40**(2), 141–147 (2012).
7. E. Spoerl, M. Huhle, and T. Seiler, "Induction of cross-links in corneal tissue," *Exp. Eye Res.* **66**(1), 97–103 (1998).
8. E. Sporl et al., "[Increased rigidity of the cornea caused by intrastromal cross-linking]," *Der Ophthalmologe: Zeitschrift der Deutschen Ophthalmologischen Gesellschaft* **94**(12), 902–906 (1997).
9. A. Caporossi et al., "Long-term results of riboflavin ultraviolet a corneal collagen cross-linking for keratoconus in Italy: the Siena eye cross study," *Am. J. Ophthalmol.* **149**(4), 585–593 (2010).
10. F. Raiskup-Wolf et al., "Collagen crosslinking with riboflavin and ultraviolet-A light in keratoconus: long-term results," *J. Cataract Refract. Surg.* **34**(5), 796–801 (2008).
11. P. Vinciguerra et al., "Intraoperative and postoperative effects of corneal collagen cross-linking on progressive keratoconus," *Arch. Ophthalmol.* **127**(10), 1258–1265 (2009).
12. R. D. Stulting, "Corneal collagen cross-linking," *Am. J. Ophthalmol.* **154**(3), 423–424 e421 (2012).
13. F. Hafezi et al., "Collagen crosslinking with ultraviolet-A and hypo-osmolar riboflavin solution in thin corneas," *J. Cataract Refract. Surg.* **35**(4), 621–624 (2009).
14. Y. A. Khan et al., "Riboflavin and ultraviolet light a therapy as an adjuvant treatment for medically refractive Acanthamoeba keratitis: report of 3 cases," *Ophthalmology* **118**(2), 324–331 (2011).
15. G. Wollensak, E. Spoerl, and T. Seiler, "Riboflavin/ultraviolet-A-induced collagen crosslinking for the treatment of keratoconus," *Am. J. Ophthalmol.* **135**(5), 620–627 (2003).
16. Y. Zhang et al., "Effect of the synthetic NC-1059 peptide on diffusion of riboflavin across an intact corneal epithelium," *Invest. Ophthalmol. Visual Sci.* **53**(6), 2620–2629 (2012).
17. M. Filippello, E. Stagni, and D. O'Brart, "Transepithelial corneal collagen crosslinking: bilateral study," *J. Cataract Refract. Surg.* **38**(2), 283–291 (2012).
18. H. U. Celik et al., "Accelerated corneal crosslinking concurrent with laser in situ keratomileusis," *J. Cataract Refract. Surg.* **38**(8), 1424–1431 (2012).
19. R. R. Krueger, J. C. Ramos-Esteban, and J. Kanellopoulos, "Staged intrastromal delivery of riboflavin with UVA cross-linking in advanced bullous keratopathy: laboratory investigation and first clinical case," *J. Refract. Surg.* **24**(7), S730–S736 (2008).
20. P. Kamaev et al., "Photochemical kinetics of corneal cross-linking with riboflavin," *Invest. Ophthalmol. Visual Sci.* **53**(4), 2360–2367 (2012).
21. D. Chai et al., "Quantitative assessment of UVA-riboflavin corneal cross-linking using nonlinear optical microscopy," *Invest. Ophthalmol. Visual Sci.* **52**(7), 4231–4238 (2011).
22. B. Bagga et al., "Endothelial failure after collagen cross-linking with riboflavin and UV-A: case report with literature review," *Cornea* **31**(10), 1197–1200 (2012).
23. C. N. LaFratta et al., "Multiphoton fabrication," *Angew. Chem.* **46**(33), 6238–6258 (2007).
24. M. Losin et al., "Microstructuration of protein matrices by laser-induced photochemistry," *J. Optoelectron. Adv. Mater.* **9**(3), 716–720 (2007).
25. B. Kaehr and J. B. Shear, "Multiphoton fabrication of chemically responsive protein hydrogels for microactuation," *Proc. Natl. Acad. Sci. U.S.A.* **105**(26), 8850–8854 (2008).
26. C. Y. Khripin, C. J. Brinker, and B. Kaehr, "Mechanically tunable multiphoton fabricated protein hydrogels investigated using atomic force microscopy," *Soft. Matter.* **6**(12), 2842–2848 (2010).
27. K. Kuetemeyer et al., "Two-photon induced collagen cross-linking in bioartificial cardiac tissue," *Opt. Express* **19**(17), 15996–16007 (2011).
28. Y. H. Bi et al., "Two-photon-excited fluorescence and two-photon spectrofluoroelectrochemistry of riboflavin," *Electron. Commun.* **8**(4), 595–599 (2006).

29. D. Karamichos, N. Lakshman, and W. M. Petroll, "An experimental model for assessing fibroblast migration in 3-D collagen matrices," *Cell Motility Cytoskeleton* **66**(1), 1–9 (2009).
30. O. N. Scott et al., "Indentation of freestanding circular elastomer films using spherical indenters," *Acta Mater.* **52**(16), 4877–4885 (2004).
31. M. Ahearne et al., "Characterizing the viscoelastic properties of thin hydrogel-based constructs for tissue engineering applications," *J. Royal Soc. Interface* **2**(5), 455–463 (2005).
32. W. R. Zipfel, R. M. Williams, and W. W. Webb, "Nonlinear magic: multiphoton microscopy in the biosciences," *Nat. Biotech.* **21**(11), 1368–1376 (2003).
33. A. Sharma et al., "Persistent corneal edema after collagen cross-linking for keratoconus," *Am. J. Ophthalmol.* **154**(6), 922–926 e1 (2012).
34. G. D. Kymionis et al., "Corneal collagen cross-linking with riboflavin and ultraviolet-A irradiation in patients with thin corneas," *Am. J. Ophthalmol.* **153**(1), 24–28 (2012).
35. P. I. Condon, M. O'Keefe, and P. S. Binder, "Long-term results of laser in situ keratomileusis for high myopia: risk for ectasia," *J. Cataract Refract. Surg.* **33**(4), 583–590 (2007).
36. M. Kohlhaas et al., "Biomechanical evidence of the distribution of cross-links in corneas treated with riboflavin and ultraviolet A light," *J. Cataract Refract. Surg.* **32**(2), 279–283 (2006).
37. T. Schilde et al., " Enzymatic evidence of the depth dependence of stiffening on riboflavin/UVA treated corneas," *Ophthalmologe* **105**(2), 165–169 (2008).
38. S. Hayes et al., "Depth profile study of abnormal collagen orientation in keratoconus corneas," *Arch. Ophthalmol.* **130**(2), 251–252 (2012).
39. K. M. Meek et al., "Changes in collagen orientation and distribution in keratoconus corneas," *Invest. Ophthalmol. Vis. Sci.* **46**(6), 1948–1956 (2005).
40. L. P. Cui et al., "High-resolution, noninvasive, two-photon fluorescence measurement of molecular concentrations in corneal tissue," *Invest. Ophthalmol. Visual Sci.* **52**(5), 2556–2564 (2011).
41. M. Ahearn et al., "Mechanical characterization of biomimetic membranes by micro-shaft poking," *J. Royal Soc. Interface* **6**(34), 471–478 (2009).
42. H. Studer et al., "Biomechanical model of human cornea based on stromal microstructure," *J. Biomech.* **43**(5), 836–842 (2010).